Journal of Physics: Conference Series **547** (2014) 012021 doi:10.1088/1742-6596/547/1/012021

On the effective thermal conductivity of metal foams

Paola Ranut and Enrico Nobile

Department of Engineering and Architecture, University of Trieste, Piazzale Europa 1, 34127 Trieste (Italy)

E-mail: pranut@units.it

Abstract. Knowing the effective thermal conductivity is essential in order to design a metal foam heat transfer device. Beside the experimental characterization tests, this quantity can be deduced from empirical correlations and theoretical models. Moreover, CFD (Computational Fluid Dynamics) and numerical modeling in general, at the pore scale, are becoming a promising alternative, especially when coupled with a realistic description of the foam structure, which can be recovered from X-ray computed microtomography (μ-CT). In this work, a review of the most relevant correlations and models published in the literature, usable for the estimation of the effective thermal conductivity of metal foams, will be outlined. In addition, a validation of the models with the experimental values available in the literature will be presented, for both air and water as working fluids. Furthermore, the results of a strategy based on μ-CT - CFD coupling at the pore level will be illustrated.

1. Introduction

In the last decades, research in flow and heat transfer in porous media has received increased attention, in view of the broad range of applications that they find in science and engineering. Porous media are employed, for instance, in packed and fluidized beds, catalytic converters, filtration equipments, light-weight structural panels, heat and energy absorption devices. In recent years, high-porosity metal foam materials have caught the attention in view of their low density and peculiar transport properties, which make them attractive for enhancing the thermal performances of heat transfer devices, while allowing the use of smaller and lighter equipments. Most common metal foams are made of aluminum and copper alloys. Usually, their porosity ε, i.e., the volume fraction occupied by the voids, falls between 80% to 97%, while the pore density of uncompressed open-cell foams ranges from 5 to 100 PPI (pores per inch). The cross section of the solid ligaments varies according to the porosity, from an inner concave triangle at $\varepsilon = 0.97$ to a circle at $\varepsilon = 0.85$. In relation to heat transfer, the attractiveness of metal foams derives from their specific geometric structure, as the high surface area to volume ratio, the high conductivity of the solid matrix and the enhanced flow mixing induced by the tortuous flow paths, which is sometimes referred to as thermal dispersion.

In order to effectively utilize metal foams in heat transfer applications, accurate knowledge of their thermal transport properties are needed. From a practical point of view, it is common to assimilate the foam to a homogeneous medium having an effective thermal conductivity k_{eff} which depends, to varying degrees, on conduction in both the solid and fluid phase, convection and radiation [1]. Conduction in the solid phase is the principal heat transfer modality, even in the case of less conducting solid matrices. As Calmidi and Mahajan [2] observed, the role

of thermal dispersion induced by hydrodynamic phenomena can be considerable for water-foam systems but it is almost negligible in the case of air-foam systems in view of the relatively high conductivity of the solid phase. Furthermore, at high temperatures, the effective thermal conductivity may depend even on radiation. The simplest heat transfer mechanism in a porous medium involves only conduction and occurs when the fluid inside is stagnant. In this case, the energy transport is controlled by the so called effective stagnant thermal conductivity, or effective thermal conductivity hereafter.
Interest in heat transfer in porous media dates back to the 19th century. Since Maxwell's work in 1865, there have been many efforts to estimate the effective thermal conductivity but, despite the constant advances, the problem is still open. Among the large amount of works about porous media, several papers provide relations specifically derived for metal foams, in which convection and thermal radiation are neglected. According to the methodology followed, these works can be classified as (1) asymptotic solutions, (2) empirical correlations and (3) unit cell approaches. In addition, the literature offers several contributions in which the effective thermal conductivity is estimated numerically, both on simplified models [3] and realistic geometries [1, 4, 5].
The paper is organized in the following way. In Sec. 2, a review of the most significant empirical and analytical models for the estimation of the effective thermal conductivity of metal foams, summarized in Table 1, is described. In Sec. 3, the results of three characterization tests based on a μ-CT - CFD strategy, involving numerical simulations at the pore level, are illustrated.
It is worth pointing out that not all the models delineated in Sec. 2 were developed directly for metallic foams. The literature includes further models which have not been considered here since they should be optimized before being applied to metal foams. For the model illustrated, the predicting capabilities have been tested against a wide set of experimental values taken from the literature, which comprises data for both air and water [6–9]. The RMS values reported in Table 1 corresponds to the mean square error between the available experimental data and the values calculated with the model.

2. Available models for the effective thermal conductivity

2.1. Asymptotic solutions

This group incorporates the theoretical correlations corresponding to two limiting cases for the effective conductivity, called upper and lower bounds.
The Parallel model $k_{||}$, Eq. (1), is an upper bound which combines the thermal conductivity of the solid, k_s, and the fluid, k_f, in an arithmetic mean, through the volume fractions of the two phases. The lower bound Series model, $k_{\perp}$, Eq. (2), is obtained by arranging k_s and k_f in series. Two other limiting solutions exist, the Maxwell-Eucken correlations, Eq. (3) and Eq. (4), originally formulated for a solid medium having a random distribution of small spheres
As it can be appreciated from Table 1, these asymptotic solutions are not suited for describing the real trend of the experimental data.

2.2. Empirical correlations

This category comprises the relations obtained by fitting experimental data. Their ability to accurately describe the behaviour of metal foams is often demanded to the fitting parameters, whose values can be calibrated over the experimental measurements available.
Calmidi and Mahajan [6] formulated an alternative of the parallel model, as described in Eq. (5). The values of the constants A and n were calibrated on their experimental data on aluminum foams, having porosities higher than 0.90. Equation (5) fits well the available experimental data [6–9] with a RMS of 0.309% for air and 0.180% for water.
Bhattacharya et al. [10] combined the Series and the Parallel models in Eq. (6), for which the value of the constant A was estimated after a fitting with the data of Ref. [6] and with new data

on reticulated vitreous carbon foams. Equation (6) gives a RMS of 0.360% and 0.353% when applied to air and water, respectively.
Also Singh and Kasana [11] expressed the effective thermal conductivity as a combination of $k_{||}$ and $k_{\perp}$, Eq. (7). The parameter F, corresponding to the fraction of solid oriented in the direction of the heat flow, comprises an empirical constant, whose value was calibrated over the data of Ref. [10]. This model produces a RMS of 0.329% and 0.038% in the case of air and water, respectively.
Krupiczka, reported from Ref. [12], formulated an empirical correlation, Eq. (8), for packed beds of spherical particles. Unfortunately, as can be appreciated from Table 1, this expression can not be applied satisfactorily to metal foams.
In addition, even if it seems not to work for metal foams, it is worth mentioning the work of Wang et al. [13], who expressed the effective thermal conductivity of complex materials by combining some basic structural models (Series, Parallel, Maxwell upper and lower bound, and the so called Effective Medium Theory) through combinatory rules based on structure volume fractions.

2.3. Unit cell approaches

Fall in this group the theoretical models formulated on an idealized and simplified foam geometry. In this case it is customary to model only a single unit cell, which is assumed to repeat itself throughout the medium in view of periodicity.
Calmidi and Mahajan [6] used a two-dimensional array of hexagonal cells, with square lumps of metal at the intersection of the ligaments. The geometry is constituted of three layers in series, within which the solid and fluid phase are arranged in parallel. The resulting equation for k_{eff}, Eq. (9), fits well the experimental data with a RMS of 0.330% and 0.048% for air and water, respectively.
Boomsma and Poulikakos [14] followed a strategy similar to [6], by using a 3D tetrakaidecahedron cell, made of four distinct layers in series. The ligaments had cylindrical cross section and cubic nodes are considered at their intersection. The model presents a parameter, to be estimated from the experimental data. However, Dai et al. [15] detected some errors in their development and presentation: with their corrections, the predictive capability of the model worsen significantly. Even if omitted in [16], the optimal value of the fitting parameter for the revised model leads to an unfeasible geometry. For this reason, the model is not reported in Table 1.
Jagjiwanram and Singh [17] considered a cubic unit cell having, at each vertex, one eighth of an ellipsoidal inclusion. The model, Eq. (10), presents a porosity-correction term F, which depends on two constants, C_1 and C_2, calibrated over the experimental data of Ref. [10]. A careful analysis of [17] shows that there is a typing error in reporting the value of C_2 for water: the proposed value of 0.1535 must be replaced with 0.5134. In this way the predicted values agree with those reported by the authors. The RMS of the fitting is, for air, 2.445% and, for water, 0.159%.
A cubic unit cell with cylindric struts and square lumps of metal at their intersection was used by Edouard [18]. The model can account for two different foams structures, namely fat and slim, as shown in Eq. (11), depending on whether there is accumulation of material at the struts' connections. The value of $1 - \varepsilon$ was derived for a regular pentagonal dodecahedral cell having triangular struts, reported in Ref. [19]. The predicting capability of the model is quite scarce: in the case of the fat model, the RMS is 1.847% in the case of air and 2.616% for water.
A different approach was followed by Fourie and Du Plessis [20], under the assumption of thermal nonequilibrium: empirical correlations were developed after having computed numerically the temperature field in a 3D unit cell, constituted by three mutually perpendicular solid square prisms. The proposed correlations account both of the effective (k_{ss}, k_{ff}) and the coupled (k_{fs}, k_{sf}) thermal conductivities of the medium. Coupled conductivities are considered since,

in the case of thermal nonequilibrium, conduction within a phase is function of the local mean temperature gradients of both phases. Their correlations presents a RMS of 1.495% when applied to air, and 0.657% in the case of water.
In addition to the aforementioned models, specifically formulated for metal foams, in the literature there are other works which consider other types of porous media. As an example, Schuetz and Glicksmann developed an analytical model for high-porosity polymeric foams ($\varepsilon > 0.95$), reported in Ref. [21], in which the only structural parameters are the porosity and the fraction of solid phase in the struts, f_s. As it can be seen from Eq. (13), the model resembles the Parallel model, Eq. (1), with the exception of the multiplicative factor. Although quite simple, the predictive capability of this model for metal foams is rather good: the RMS of the fitting is 0.257% and 0.414% for air and water, respectively.
Dul'nev [22] proposed a model, Eq. (14), for disperse solid systems, based on a cubic unit cell formed by 12 solid prisms of square section. This model fits the experimental data with a RMS of 0.795% in the case of air, and 0.340% in the case of water.
Ahern et al. [21] developed a correlation, based on the Maxwell relation for mixtures of materials having different electrical conductivities, Eq. (15), as function of the fraction of solid in the faces (called windows by the authors), f_w. If applied to the available data set, the RMS of the fitting is 0.258% for air and 0.345% for water.

A graphical comparison of the most effectual models for the effective thermal conductivity is illustrated in Fig. 1 and Fig. 2.

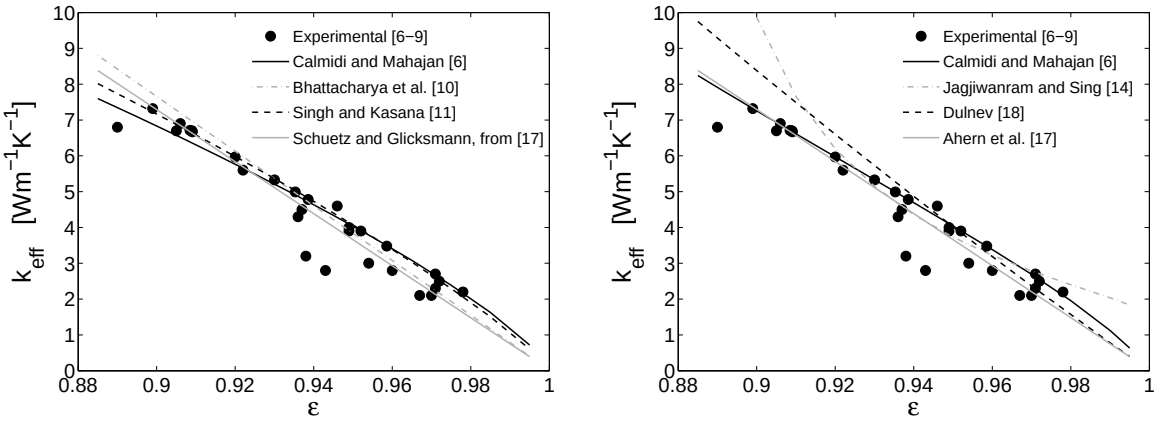

(a) (b)

Figure 1: Validation of the models for the prediction of the effective thermal conductivity in the case of air.

Table 1: Available models for effective thermal conductivity. (A) stands for air while (W) for water.

Authors	**Model**		**RMS** (%)
	Asymptotic solutions		
Parallel model	$k_{\|\|} = \varepsilon k_f + (1-\varepsilon)k_s$	(1)	15.23 (A) 67.64 (W)
Series model	$k_\perp = \left(\frac{\varepsilon}{k_f} + \frac{1-\varepsilon}{k_s}\right)^{-1}$	(2)	22.36 (A) 19.70 (W)

Table 1: continues in the next page.

Table 1: continues from the previous page

Authors	**Model**		**RMS** (%)
Maxwell upper bound	$k_{\text{eff}} = k_s \dfrac{2k_s + k_f - 2(k_s - k_f)\varepsilon}{2k_s + k_f + (k_s - k_f)\varepsilon}$	(3)	26.79 (A) 14.33 (W)
Maxwell lower bound	$k_{\text{eff}} = k_f \dfrac{3k_s - 2(k_s - k_f)\varepsilon}{3k_f + (k_s - k_f)\varepsilon}$	(4)	22.33 (A) 19.04 (W)
	Empirical correlations		
Calmidi and Mahajan [6]	$k_{\text{eff}} = \varepsilon k_f + A(1-\varepsilon)^n k_s$ $A = 0.181, n = 0.763$	(5)	0.309 (A) 0.180 (W)
Bhattacharya et al. [10]	$k_{\text{eff}} = Ak_{\|\|} + (1-A)k_\perp$ $A = 0.35$	(6)	0.360 (A) 0.239 (W)
Singh and Kasana [11]	$k_{\text{eff}} = k_{\|\|}^F k_\perp^{1-F}$ $F = C\left[0.3031 + 0.0623 \ln\left(\varepsilon k_s/k_f\right)\right]$ $0 \le F \le 1$, $C = 0.9683$ (A), $C = 1.0647$ (W)	(7a) (7b)	0.329 (A) 0.038 (W)
Krupiczka, from Ref. [12]	$k_{\text{eff}} = k_f \left(\dfrac{k_s}{k_f}\right)^{0.28 - 0.757\log\varepsilon - 0.057\log\left(k_s/k_f\right)}$ Developed for packed beds of spherical particles	(8)	21.13 (A) 16.601 (W)
	Analytical models		
Calmidi and Mahajan [6]	$k_{\text{eff}} = \left(\dfrac{2}{\sqrt{3}}\left(\dfrac{r\frac{b}{L}}{k_f + \left(1+\frac{b}{L}\right)\frac{k_s - k_f}{3}} + \dfrac{(1-r)\frac{b}{L}}{k_f + \frac{2}{3}\frac{b}{L}\left(k_s - k_f\right)} + \dfrac{\frac{\sqrt{3}}{2} - \frac{b}{L}}{k_f + \frac{4r}{3\sqrt{3}}\frac{b}{L}\left(k_s - k_f\right)}\right)\right)^{-1}$ $\dfrac{b}{L} = \dfrac{-r + \sqrt{r^2 + \frac{2}{\sqrt{3}}(1-\varepsilon)\left(2 - r\left(1 + \frac{4}{\sqrt{3}}\right)\right)}}{\frac{2}{3}\left(2 - r\left(1 + \frac{4}{\sqrt{3}}\right)\right)}$ $r = 0.09$, $r = t/b < 0.0336$, b: half thickness of the lump, L: length of the strut, t: half thickness of the strut	(9a) (9b)	0.330 (A) 0.048 (W)
Jagjiwanram and Singh [17]	$k_{\text{eff}} = \dfrac{k_f\left[(k_s - k_f)\sqrt{\pi/6}\sqrt{F} + k_f\right]}{k_f + (1 - \sqrt{6/\pi}\sqrt{F})(k_s - k_f)\sqrt{\pi/6}\sqrt{F}}$ $\sqrt{F} = C_1\sqrt{1-\varepsilon}\exp(k_f/k_s) + C_2$ $C_1 = 0.034, C_2 = 0.7111$ (A) $C_1 = 0.5217, C_2 = 0.5135$ (W)	(10a) (10b)	2.45 (A) 0.159 (W)

Table 1: continues in the next page.

Table 1: continues from the previous page

Authors	**Model**	**RMS** (%)
Edouard [18]	$$\frac{1}{k_{\text{eff}}} = \frac{2d}{(d^2(4y^2-2\pi y)+\pi d)k_s + (d^2(2\pi y-4y^2)-\pi d+1)k_f} + \frac{2d(y-1)}{4y^2d^2k_s+(1-4y^2d^2)k_f} + \frac{1-2dy}{\pi d^2 k_s+(1-\pi d^2)k_f} \quad (11a)$$ $$1-\varepsilon = \underbrace{3\pi d^2(1-2d)+8d^3}_{A} + \underbrace{\delta d^3(8\delta^2+24\delta+24-6\pi)}_{B} \quad (11b)$$ $$\text{If } \delta = 0: \quad A = k^2\frac{\sqrt{15}}{\phi^4} - k^3\frac{\sqrt{10}}{3\phi^4} \quad (11c)$$ $$\text{If } \delta \neq 0: \begin{cases} A = k^2\frac{\sqrt{15}}{\phi^4} - k^3\frac{\sqrt{10}}{3\phi^4} \\ B = \frac{40}{\sqrt{5}\phi^4}\frac{\sin^2(\frac{\pi}{5})\phi^2\left(1-\frac{k}{2}\sqrt{\frac{2}{3}}\right)}{32\sqrt{3}(3-\phi)}\sqrt{\frac{1}{4}-\frac{\sin^2(\frac{\pi}{5})\phi^2}{9-3\phi}} \\ \quad + \frac{12k}{\sqrt{5}\phi^2}\left(\frac{5\phi}{4\sqrt{3-\phi}} - \frac{\pi}{4}\frac{\phi^2}{3-\phi}\right)\left(1-\frac{k}{2}\sqrt{\frac{2}{3}}\right)^2 \end{cases} \quad (11d)$$ $d = b/L$, $y = x/b = 1+\delta$, $\delta \geq 0$, $\phi = 1.618$ b: radius of the cylindric strut, L: lenght of the cylindric strut, x: length of the square lump, k: ratio between strut side and the side of a perfect pentagon	For $\delta \neq 0$: 1.847 (A) 2.616 (W)
Fourie and Du Plessis [20]	$$k_{\text{eff}} = (1-\varepsilon)(k_{ss}+k_{fs}) + \varepsilon(k_{sf}+k_{ff}) \quad (12a)$$ $$k_{ss} = 0.559(1.64-\varepsilon)k_s + 0.562k_f\left(\frac{\varepsilon}{1-\varepsilon}\right)^{0.235} \quad (12b)$$ $$k_{sf} = 1.18k_f\varepsilon^2 - 2.51k_f\varepsilon + 1.32k_f \quad (12c)$$ $$k_{ff} = 0.645(\varepsilon-0.961)(k_f^2/k_s) + 1.82k_f\varepsilon^2 - 3.29k_f\varepsilon + 2.43k_f \quad (12d)$$ $$k_{fs} = (k_f^2/k_s)(-14.2\varepsilon^2+22.6\varepsilon-9.62) + 0.328k_f\left(\frac{\varepsilon}{1-\varepsilon}\right)^{0.539} \quad (12e)$$ Under thermal nonequilibrium conditions	1.495 (A) 0.657 (W)
Schuetz and Glicksmann, from Ref. [21]	$$k_{\text{eff}} = \varepsilon k_f + (1-\varepsilon)\frac{2-f_s}{3}k_s \quad (13)$$ Derived for polimeric foams. For metal foams, $f_s = 1$	0.257 (A) 0.406 (W)
Dulnev [22]	$$k_{\text{eff}} = k_s t^2 + k_f(1-t)^2 + \frac{2t(1-t)k_f k_s}{k_s(1-t)+k_f t} \quad (14a)$$ $$t = \frac{1}{2} + \cos\left(\frac{1}{3}\arccos(2\varepsilon-1)+\frac{4\pi}{3}\right) \quad (14b)$$ t: dimensionless thickness of the solid ligament	0.795 (A) 0.340 (W)
Ahern et al. [21]	$$k_{\text{eff}} = k_f + (k_s-k_f)(1-\varepsilon)\beta \quad (15a)$$ $$\beta = f_w\beta_w + (1-f_w)\beta_s \quad (15b)$$ $$\beta_s = \frac{1}{3}\left(1+\frac{4k_f}{k_f+k_s}\right), \quad \beta_w = \frac{2}{3}\left(1+\frac{k_f}{2k_s}\right) \quad (15c)$$ $f_w = 1-f_s$: fraction of solid in the windows. For metal foams, $f_w = 0$	0.258 (A) 0.345 (W)

Table 1: end

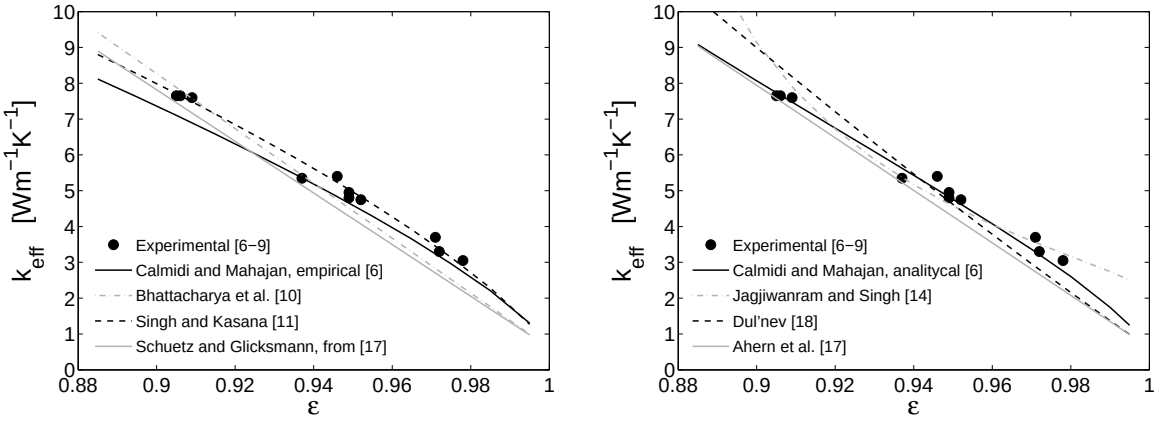

(a) (b)

Figure 2: Validation of the models for the prediction of the effective thermal conductivity in the case of water.

3. Microtomography-CFD based approach

Besides the models illustrated so far, the literature offers several examples in which the effective thermal conductivity is estimated, numerically, by means of CFD. In order to perform a numerical simulation, the foam structure can be idealized [3, 23, 24] or described in a realistic way [1, 4, 25, 26]. In the second case, the foam geometry can be recovered, with high fidelity, after a X-ray microtomography (μ-CT) scan, as described in [1]. The result of a μ-CT is a series of 2D X-ray images, recorded during a 360° rotation of the sample around its vertical axis, which can be afterwards combined together in order to obtain a 3D volume. The elemental digital units constituting this reconstructed volume are called voxels.

In [1], three aluminum foams samples of different pore densities (10-20-30 PPI) were analyzed by means of the combined methodology X-ray μ-CT - CFD. The tomographic scan, of 9.1 µm-resolution, was performed at the *TomoLab station* [27] of the Elettra Synchrotron Light Laboratory in Trieste. It should be emphasized that the chosen resolution is significantly higher, at least twice, than most of the studies published in the literature [4, 25, 26, 28, 29].

The domains used for the CFD simulations are a fraction of the volume reconstructed from the μ-CT; the dimensions of the computational domains are chosen according to the PPI of the foam: 548^3 voxels for the 30 PPI sample, 848^3 for the 20 PPI sample and 1000^3 for the 10 PPI one. The commercial software ANSYS ICEM CFD was employed for the generation of geometrically exact, feature-preserving grids: in view of the complexity of the geometry, a tetrahedral grid was employed.

The CFD simulations were performed with ANSYS CFX 13.0. In this case, the problem was only conductive since the interstitial fluid (air or water) was considered as motionless. The energy equation was solved both in the fluid and in the solid region. An arbitrary temperature difference was applied along one direction, while the other lateral faces were kept adiabatic. The simulations were performed along the three space directions, in order to test the degree of isotropy of the medium.

The effective thermal conductivity was computed as:

$$k_{\text{eff}} = \frac{-\int \mathbf{J} \cdot d\mathbf{A}}{\frac{\partial T}{\partial x_i} A} = \frac{-\left(\int_s \mathbf{J} \cdot d\mathbf{A}_s + \int_s \mathbf{J} \cdot d\mathbf{A}_f\right)}{\frac{\partial T}{\partial x_i} (A_s + A_f)} \tag{16}$$

where **J** and $d\mathbf{A}$ are the heat flux and the outward pointing area vector, respectively, and the subscripts s and f refer to the solid and the fluid.
The simulations demonstrated that the degree of isotropy of the medium is related to the pore density of the sample. In fact, while for the 30 PPI foam the thermal conductivities evaluated along the three spatial directions are quite close, for the other two samples the differences are more significant. There are two possible explanations for this behaviour. The first is the peculiar and different geometrical characteristics of the samples. In fact, while the cells of the 30 PPI sample are almost visually identical along the three spatial coordinates, for the other two samples they are rather stretched along one specific direction. The highest value of k_{eff} is registered precisely along the direction of elongation of the cells. In addition, as already asserted in [4], this anisotropy might be affected by the size of the domains employed. However, 9.1 μm resolution limited the maximum size of the scanned samples and precluded the employment of significantly larger domains in the CFD simulations. Therefore, in view of these considerations, and following the example of [4], in Table 2 only the mean values of k_{eff}, averaged along the three spatial coordinates, are summarized. A graphical comparison with the experimental and numerical values published in the literature is reported in Figure 3.
As it can be seen, the values of k_{eff} evaluated in this study agree well with those available in the literature. The values of k_{eff} estimated with water are slightly larger than those with air, thus proving that, for aluminum foams, the thermal conductivity of the fluid influences, but not in a significant way, the effective thermal conductivity of the medium.

Table 2: Prediction of the effective thermal conductivity values [$\text{Wm}^{-1}\text{K}^{-1}$] with air or water as the interstitial fluid.

PPI	Porosity	$k_{\text{eff,air}}$	$k_{\text{eff,water}}$
10	0.944	3.49	4.13
20	0.927	4.97	5.76
30	0.929	5.31	5.99

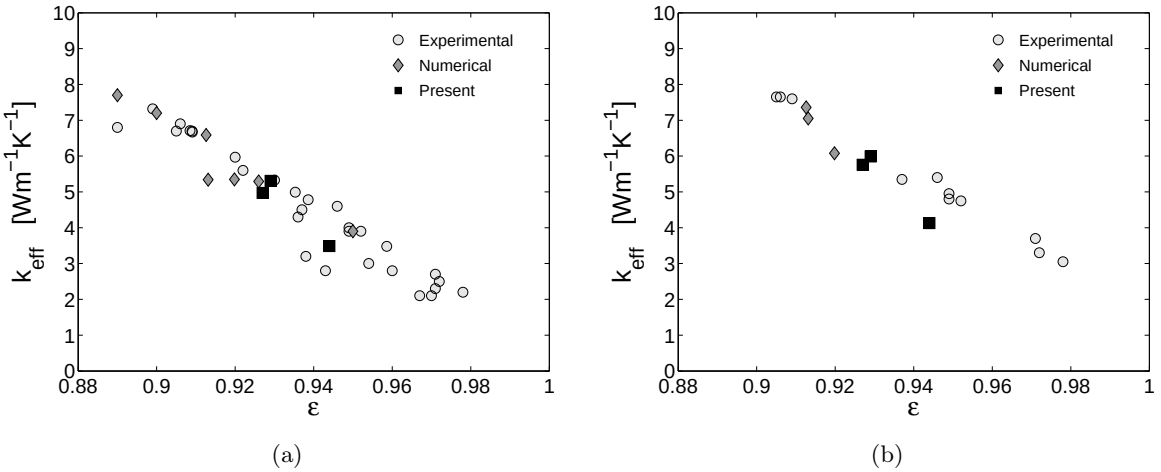

Figure 3: Comparison of the values of the effective thermal conductivity calculated numerically by the present authors with the experimental and numerical data available in the literature. (a) Air and (b) Water.

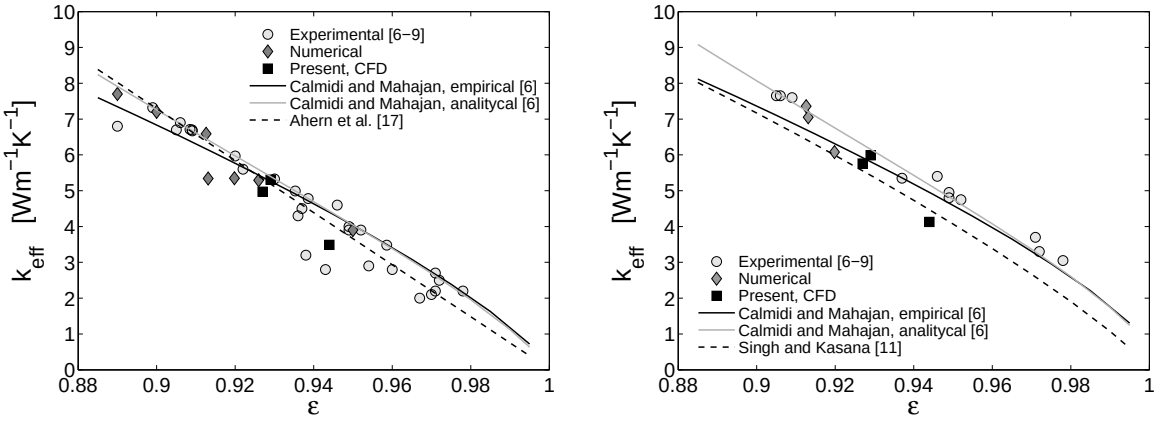

(a) (b)

Figure 4: Comparison of the values of the effective thermal conductivity calculated numerically by the present authors with the experimental and numerical data available in the literature and some of the best models described in Sec. 2. (a) Air and (b) Water.

4. Comments and concluding remarks

In this paper, the most significant models published in the literature for the estimation of the effective thermal conductivity k_{eff} of open-cell metal foams have been tested against a wide set of experimental data. From the results obtained, the following conclusions can be drawn:

- The analysis has shown that the use of a more complex theoretical approach does not always lead to better results than those estimated with an empirical model. In fact, if one considers the empirical and the analytical models of Calmidi and Mahajan [6], it can be observed that their predictions are quite similar (RMS = 0.309% vs RMS = 0.330% in the case of air, and 0.180% vs 0.048% in the case of water). On the contrary, the derivation of a theoretical model is significantly more laborious than the definition of an empirical model.
- In Fig. 4 the values of k_{eff} estimated with a combined μ-CT - CFD strategy are compared against the models, introduced in Sec. 2, which provided the best results for open-cell metal foams. As it can be seen, although the best models are generally satisfactory in predicting k_{eff}, for some applications the accuracy may not be adequate: in these cases, therefore, the proposed μ-CT - CFD strategy seems to be the best choice. However, it is considerably time and resource consuming and, therefore, its application is justified only when higher accuracy is required or, together with experimental measurements, for the validation and/or calibration of simpler models.
- In view of their greater simplicity, empirical models are sufficient, for most applications, to obtain satisfactory estimates of the effective thermal conductivity of metal foams, without resorting to complex geometrical and mathematical descriptions, leaving the μ-CT - CFD methods to specific cases where higher accuracy is required.

Acknowledgment

This work was financially supported by Italian government, MIUR grant PRIN-2009KSSKL3.

NOMENCLATURE

A Area, see Eq. (16)
$d\mathbf{A}$ Outward pointing area vector, see Eq. (16)

$\mathbf{J}$ Heat flux vector, see Eq. (16)
k_f Thermal conductivity of the fluid phase
k_{eff} Effective thermal conductivity of the foam
k_s Thermal conductivity of the solid phase
$k_{||}$ Thermal conductivity given by k_f and k_s arranged in parallel
$k_{\perp}$ Thermal conductivity given by k_f and k_s arranged in series
T Temperature, see Eq. (16)
x Generic space coordinate, see Eq. (16)
ε Porosity of the foam (fraction volume of the fluid phase)

References

[1] Ranut P, Nobile E and Mancini L 2014 *Appl. Therm. Eng.* **69** 230–240
[2] Calmidi V and Mahajan R 2000 *ASME J. Heat Transf.* **122** 557–565
[3] Krishnan S, Murthy J and Garimella S 2006 *ASME J. Heat Transf.* **128** 793–799
[4] Bodla K, Murthy J and Garimella S 2010 *Numer. Heat. Tr. A-APPL* **58** 527–544
[5] Bianchi E, Heidig T, Visconti C, Groppi G, Freund H and Tronconi E 2012 *Chem. Eng. J.* **198-199** 512–528
[6] Calmidi V and Mahajan R 1999 *ASME J. Heat Transf.* **121** 466–471
[7] Bhattacharya A and Mahajan R 2006 *J. Electron. Packaging* **128** 259–266
[8] Paek J, Kang B, Kim S and Hyun J 2000 *Int. J. Thermophys.* **21** 453–464
[9] Takegoshi E, Hirasawa Y, Matsuo J, and Okui K 1992 *Trans. Jpn. Soc. Mech. Eng.* **58(547B)** 879–884 in Japanese
[10] Bhattacharya A, Calmidi V and Mahajan R 2002 *Int. J. Heat Mass Tran.* **45** 1017–1031
[11] Singh R and Kasana H 2004 *Appl. Therm. Eng.* **24** 1841–1849
[12] Kaviany M 1999 *Principles of Heat Transfer in Porous Media* 2nd ed (Springer)
[13] Wang J, Carson J, North M and Cleland D 2006 *Int. J. Heat Mass Transfer* **49** 3075–3083
[14] Boomsma K and Poulikakos D 2001 *Int. J. Heat Mass Tran.* **44(4)** 1827–836
[15] Dai Z, Nawaz K, Park Y, Bock J and Jacobi A 2010 *Int. Commun. Heat Mass* **37** 575–580
[16] Boomsma K and Poulikakos D 2011 *Int. J. Heat Mass Tran.* **54(1)** 746–748
[17] Jagjiwanram and Singh R 2004 *Bull. Mater. Sci.* **27(4)** 373–381
[18] Edouard D 2011 *AIChE Journal* **57(6)** 1646–1651
[19] Truong Huu T, Lacroix M, Pham Huu C, Schweich D and Edouard D 2009 *Chem. Eng. Sci.* **64** 5131–5142
[20] Fourie J and Du Plessis J 2005 *AIChE Journal* **50(3)** 547–556
[21] Ahern A, Verbist G, Waire D, Phelan R and Fleurent H 2005 *Colloids and Surfaces A: Psycochem. Eng. Aspects* **263** 275–279
[22] Dul'nev G 1965 *J. Eng. Phys. Thermophys.* **9** 399–404
[23] Boomsma K, Poulikakos D and Ventikos Y 2003 *Int. J. Heat Fluid Flow* **24** 825–834
[24] Kopanidis A, Theodorakakos A, Gavaises E and Bouris D 2010 *Int. J. Heat Mass Tran.* **53** 2539–2550
[25] Petrasch J, Meier F, Friess H and Steinfeld A 2008 *Int. J. Heat Fluid Flow* **29** 315–326
[26] Gerbaux O, Buyens F, Mourzenko V, Memponteil A, Vabre A, Thovert J F and Adler P 2010 *J. Colloid Interface Sci.* **35** 155–165
[27] `http://www.elettra.trieste.it/lightsources/labs-and-services/tomolab/tomolab.html`

[28] Laschet G, Sauerhering J, Reutter O, Fend T and Scheele J 2009 *Comp. Mat. Sc.* **45** 597–603
[29] Magnico P 2009 *Chem. Eng. Sc.* **64** 3564–3575